A Numerical Case Study on a Mesoscale Convective System over the Qinghai-Xizang (Tibetan) Plateau

ZHU Guofu[*][1] (朱国富) and CHEN Shoujun[2] (陈受钧)

[1] Chinese Academy of Meteorological Sciences, Beijing 100081

[2] National key Laboratory for the Severe Storm Research (LSSR), Peking University, Beijing 100871

ABSTRACT

A mesoscale convective system (MCS) developing over the Qinghai-Xizang Plateau on 26 July 1995 is simulated using the fifth version of the Penn State-NCAR nonhydrostatic mesoscale model (MM5). The results obtained are inspiring and are as follows. (1) The model simulates well the largescale conditions in which the MCS concerned is embedded, which are the well-known anticyclonic Qinghai-Xizang Plateau High in the upper layers and the strong thermal forcing in the lower layers. In particular, the model captures the meso-α scale cyclonic vortex associated with the MCS, which can be analyzed in the 500 hPa observational winds; and to some degree, the model reproduces even its meso-β scale substructure similar to satellite images, reflected in the model-simulated 400 hPa rainwater. On the other hand, there are some distinct deficiencies in the simulation; for example, the simulated MCS occurs with a lag of 3 hours and a westward deviation of 3–5° longitude. (2) The structure and evolution of the meso-α scale vortex associated with the MCS are undescribable for upper-air sounding data. The vortex is confined to the lower troposphere under 450 hPa over the plateau and shrinks its extent with height, with a diameter of 4° longitude at 500 hPa. It is within the updraft area, but with an upper-level anticyclone and downdraft over it. The vortex originates over the plateau, and does not form until the mature stage of the MCS. It lasts for 3-6 hours. In its processes of both formation and decay, the change in geopotential height field is prior to that in the wind field. It follows that the vortex is closely associated with the thermal effects over the plateau. (3) A series of sensitivity experiments are conducted to investigate the impact of various surface thermal forcings and other physical processes on the MCS over the plateau. The results indicate that under the background conditions of the upper-level Qinghai-Xizang High, the MCS involved is mainly dominated by the low-level thermal forcing. The simulation described here is a good indication that it may be possible to reproduce the MCS over the plateau under certain large-scale conditions and with the incorporation of proper thermal physics in the lower layers.

Key words: Qinghai-Xizang (Tibetan) Plateau, mesoscale convective system (MCS), numerical simulation

1. Introduction

A series of mesoscale convective systems (MCSs) occurred daily over the Qinghai-Xizang Plateau during 25–28 July 1995. In a previous paper (Zhu and Chen, 2003), the authors analyzed their physical characteristics and evolution based on infrared (IR) satellite imagery, their largescale meteorological conditions, and convective potential available energy (CAPE). Among them, the MCS on 26 July was the strongest one with a size and physical characteristics of IR satellite imagery similar to a Mesoscale Convective Complex (MCC) (Maddox, 1980). It formed at noon LST (0600 UTC), then built up rapidly and reached its peak in the early evening hours around 1800 LST (1200 UTC), and then decayed gradually. The results from the previous analyses showed that the MCS concerned was driven and developed by the strong low-level thermal forcing and conditional instability under the conditions of the great unique nearly-circular anticyclonic high in the upper layers. All these conditions are intimately linked with the plateau itself, characterized by relatively pure thermal effects. It follows that there are many features peculiar to the MCS over the plateau
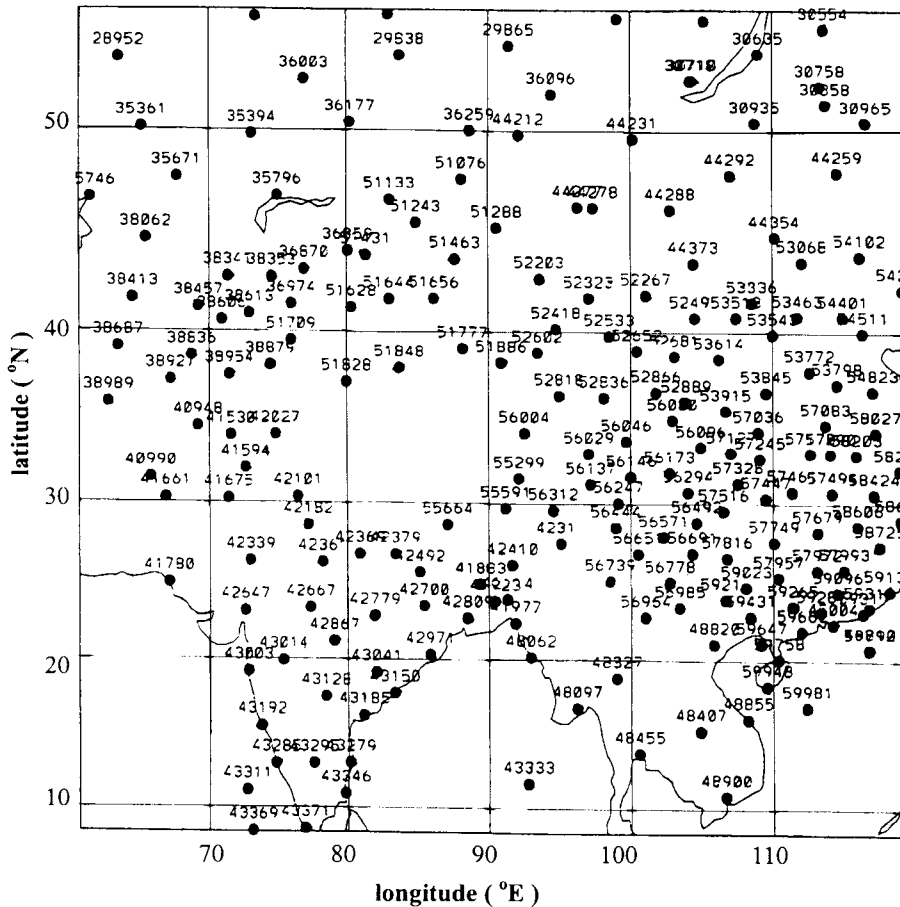
*E-mail: zhugf@cma.gov.cn

Fig. 1. Model domain and distribution of sounding observation stations (black dotted) at the initial time.

for us to study.

However, the spatial and temporal resolutions of the available observations are insufficient for studying the structure and evolution of the 26 July MCS over the plateau; in particular, there are sparse observations over the plateau, even scant data over a $10° \times 10°$ (latitude-longitude) domain in the upstream of the MCS studied west of 90°E longitude. Thereby there is a limit to the reliability of the analyses based on observations. So we must successfully simulate successfully the MCS using a sophisticated model and obtain dynamically consistent valuable high resolution output for research on the structure and evolution of the MCS. Many previous numerical studies (e.g., Anthes et al., 1982; Zhang et al., 1989) indicated that mesoscale systems can develop with initial large-scale conditions of mesoscale models. Still, since there are sparse observations, it is a challenging test to simulate the MCSs over the plateau with a meso-scale numerical model.

2. Model description and experiment design

The fifth version of the Penn State-NCAR nonhydrostatic mesoscale model (MM5) is employed for the present study. There are 23 sigma levels in the vertical direction, with a horizontal grid size of 54 km. Figure 1 shows the model domain. The model water cycles include the use of the Kain-Fritsch convective parameterization scheme (Kain and Fritsch, 1993) for the subgrid-scale moist process and the prognostic equations for resolvable cloudwater, rainwater, and graupel. A modified version of the Blackdar high-resolution Planetary Boundary Layer (PBL) parameterization (Zhang and Anthes, 1982) is used for calculation of surface vertical fluxes of sensible heat, latent heat, and momentum. For a more detailed description of MM5, the reader is referred to Grell et al. (1994).

The model is initialized at 0000 UTC 26 July 1995 with the American NCEP 2.5° (latitude-longitude)

resolution analysis, which is then enhanced by raw-insondes and surface observations. The black dots in Fig. 1 represent the observation stations at the initial time. The model is integrated for 24 hours, which covers the whole life cycle of the MCS.

In the present study, the control experiment (CNTL) is run with all of the physical processes mentioned above. Because the Qinghai-Xizang Plateau is the highest and biggest one with the most sophisticated topography and with most various surface properties in the world, a series of sensitivity experiments, including one of pseudo-adiabatic process (FDRY), and ones regardless of the surface and atmospheric radiations (NRAD), surface sensitive heat (NSEN), and surface latent heat (NLAT), respectively, are performed to investigate the impact of various surface thermal forcings and other physical processes on the MCS over the plateau. All these experiments are contained in sections 3 and 4; a summary is given in section 5 and some discussions follow in section 6.
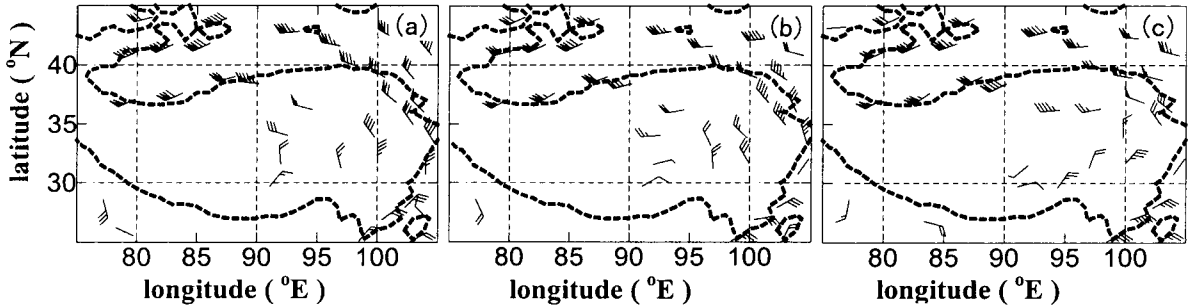
Fig. 2. Observational winds (half barb=2 m s^{-1}, flag=20 m s^{-1}) at 200 hPa at (a) 0000 UTC, (b) 1200 UTC 26, and (c) 0000 UTC 27 July.
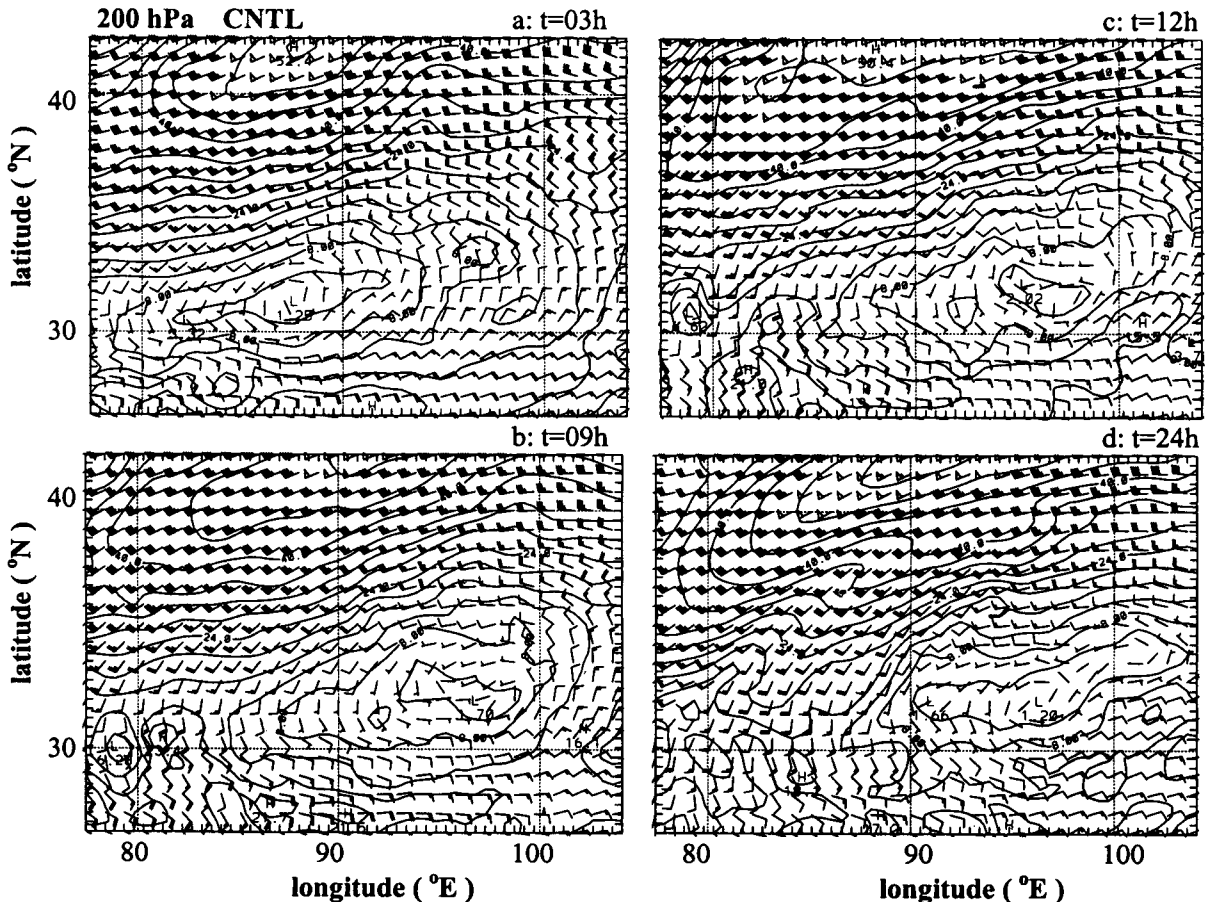
Fig. 3. CNTL forecast winds at 200 hPa at (a) t=03 h, (b) 09 h, (c) 12 h, and (d) 24 h.

The central plateau is located at about 90°E and its time difference is +6 h; for example, 0600 UTC corresponds to 12 LST (noon).

3. CNTL experiment

3.1 *CNTL-simulated large-scale environment field of the concerned MCS*

At the initial time (t=00 h, at 0000 UTC 26 July 1998) the entire plateau was occupied by a great nearly-circular anticyclone at 200 hPa (Fig. 2a), its center being west of 90°E.

Figure 3a shows the CNTL forecast winds at 200 hPa. Similar to the t=00 h wind observations (Fig. 2a), the simulated 200 hPa anticyclone at t=03 h was nearly-circular, with its center around (32°N, 87.5°E). Afterwards, it visibly shifted to the east by north, and its center arrived at about (33°N, 97°E) at t=09 h. Then the anticyclone shifted little and was rather stable during t=09 h–12 h (Figs. 3b and 3c). But its shape started to transform after t=12 h and it explicitly extended in the northeast-southwest orientation at t=24 h (Fig. 3d).

The above-mentioned evolution of the 200 hPa anticyclone over the plateau could be verified against observation winds in Fig. 2. One can see that the center of a great nearly-circular anticyclone was located west of 90°E at 0000 UTC 26 July (t=00 h), east of 90°E at 1200 UTC 26 (t=12 h), and afterwards it shifted little during 1200 UTC 26 to 0000 UTC 27 (t=12 h–24 h), but transformed after t=12 h, with a northeast-southwest orientation in shape.

Since the great anticyclone over the plateau existed as the larger-scale dynamic system of the MCS over the plateau on 26 July, the above characteristics of the CNTL-simulated 200 hPa winds reflect that the model can reproduce the largescale environment where the MCS was imbedded.

The CNTL-simulated 200 hPa westerlies in the northwestern part of the anticyclone began to strengthen after t=12 h and got a maximum speed of 57.2 m s^{-1} at t=18 h, which may indicate an impact of the developed MCS on its largescale surroundings.
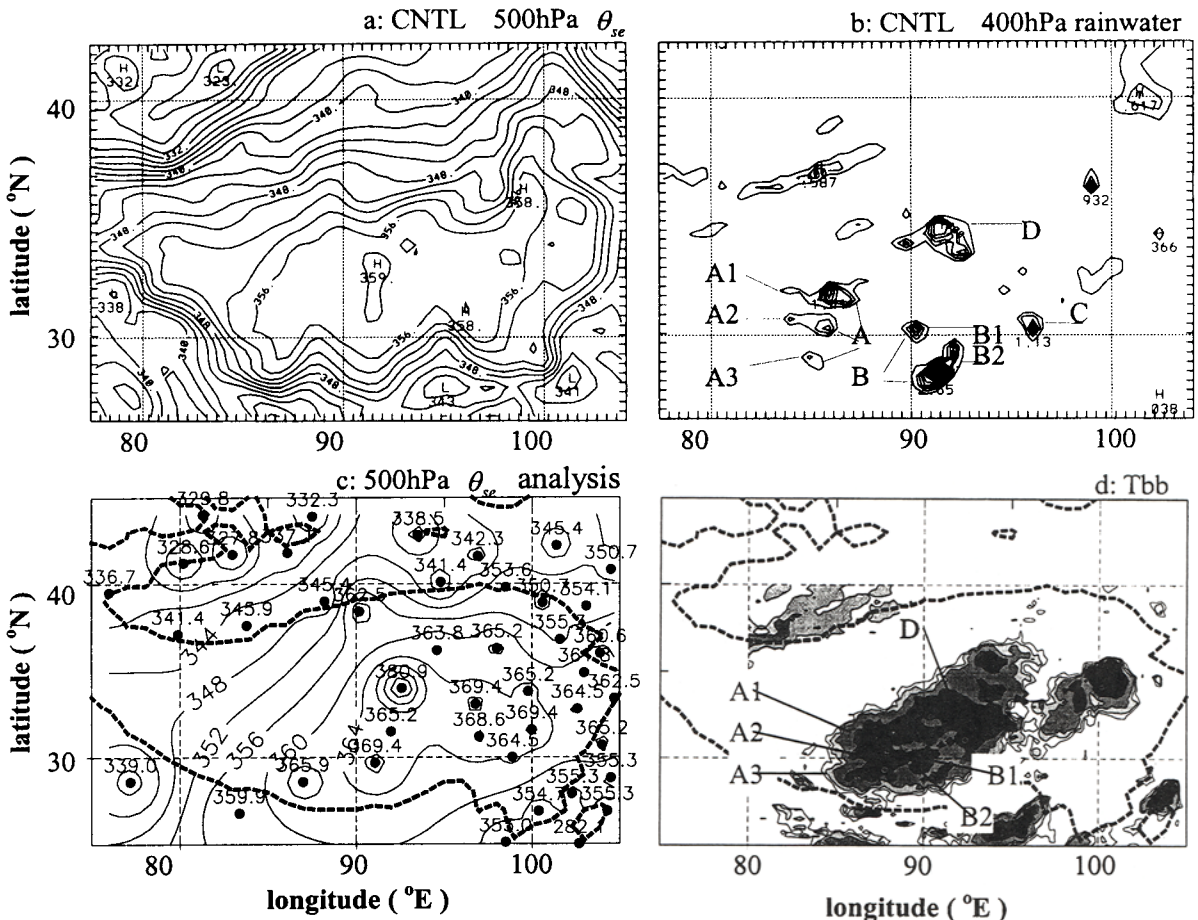

Fig. 4. (a) the model 500 hPa θ_{se} (2 K intervals), (b) the model 400 hPa rainwater mixing rate (0.2 g kg^{-1} intervals) at t=15 h, and (c) θ_{se} analysis (4 K intervals) and (d) T_{bb} map at 1200 UTC 26.

3.2 CNTL-simulated low-level thermal features associated with the MCS

The model 500 hPa pselldo-equivalent potential temperature θ_{se} at $t=15$ h (Fig. 4a) had general features similar to the θ_{se} analysis at 1200 UTC (Fig. 4c). Over the plateau is the high θ_{se} region, with two extensions of a warm tongue in its southwestern and northeastern directions (near 87°E and south of 30°N, near 100°E and north of 35°N, respectively). Its central area with a north-south orientation lay to the east of 90°E, with a maximum value in its north. There was a relatively low θ_{se} belt along 95°E in the high θ_{se} region. Furthermore, in Fig. 4a there exists a CNTL-simulated sizable northwestward extension of a warm area to the west of 90°E over the plateau, where there are no observation stations. On the other hand, in the CNTL simulation there are evident deficiencies such as a lag of 3 hours, a difference of minus 3–5 K in the high θ_{se} region over the plateau and minus 10–15 K in the θ_{se} maximum in comparison with the θ_{se} analysis.

There is a close relation between the 400 hPa rainwater and the 500 hPa θ_{se}. In Figs. 4a and 4b, it is clear that 400 hPa rainwater over the plateau formed within the 500 hPa high θ_{se} region, and each of the rainwater areas was accompanied by a high θ_{se} center or tongue: for instance, the rainwater area marked D in Fig. 4b was located within the high θ_{se} region over theplateau (Fig. 4a), and the three groups of rainwater areas marked A, B, and C (near 30°N and approximately along 86°E, 90°E, and 96°E, respectively) were each with a warm tongue of the wavelike θ_{se} contours in the south of the high θ_{se} region. In contrast, to the northwest of the plateau, the northeast-southwest orientated rainwater belt associated with the westerlies was located to the south of the strongest θ_{se} gradient, not within the high θ_{se} region.

The CNTL-simulated 400 hPa rainwater areas over the plateau exhibited to some degree the main features of the meso-β scale substructure in the mature MCS. For instance, rainwater areas A1, A2, A3, B1, B2, and D at $t=15$ h in Fig. 4b can find their counterparts in the (equivalent blackbody temperature) T_{bb} map at 1200 UTC 26 (Fig. 4d). These model rainwater areas appeared at t=09 h, though convection over the plateau in the T_{bb} map appeared at 0600 UTC 26 (figures not shown), and therefore the CNTL model has a lag of 3 hours. There are other evident deficiencies, such as errors in position, shape, and strength of A1, A2, and A3, and an error in position of D, and over-estimates in the strength and size of B2.

After all these deficiencies in the CNTL simulation, the model simulated well the low-level thermal features associated with the MCS over the plateau on 26 July, and even to some degree the meso-β scale substructure of the MCS. In addition, taking into consideration the lag of 3 hours, we can see that the model also simulated the evolution of the MCS similar to T_{bb} map. That is, its initial convective activities started by solar heating at noon LST (0600 UTC), and it reached its peak in the early evening hours around 1800 LST (1200 UTC).

3.3 CNTL-simulated mesoscale cyclonic vortex associated with the MCS

Of particular significance is that a mesoscale cyclonic vortex associated with the MCS is represented by CNTL. Its structure and evolution are undescribable for upper-air sounding data.

Figure 5 shows the CNTL-simulated 500 hPa winds and geopotential heights from $t=06$ h to 21 h every 3 h. It is clear that there was a cyclonic vortex over the western central plateau (west of 90°E) during the period of t=15 h–18 h. The vortex was circular and 4° latitude/longitude in diameter with its center around (34°N, 87°E) and had a life cycle of 3–6 hours.

This model vortex can be verified to some degree against the observations for its entity and its relationship to the concerned MCS. Figure 6 shows the 500 hPa observation winds at 1200 UTC 26 July. A meso-scale cyclonic vortex with diameter of 3–4° latitude/longitude can be analyzed around (34°N, 92°E) over the plateau in Fig. 6 for sure, and by conferring Fig. 4d we can find that the vortex is embedded in the MCS. Moreover, the pattern of the model wind field (Fig. 5d) is consistent with that from the observations (Fig. 6). Therefore, the CNTL model captured the meso-α scale characteristics of the MCS, but had a lag of 3 hours and a position windage of westward 4–5° latitude/longitude.

This meso-α scale cyclonic vortex did not form till the mature stage of the MCS, with a closed contour at $t=15$ h. Velasco and Fritsch (1987) discussed ad hoc the possible development mechanism of the mesoscale vortices of MCCs and pointed out that MCCs reflect atmospheric conditions wherein the intense deep convection occurs over a large enough area for a sufficient time to generate a mesoscale dynamic response in the form of a mesoscale warm-core vortex. In this study, the CNTL-simulated meso-α scale vortex helps to serve as another evidence for the above mechanism. Now more detailed analyses of the evolution and structure of this meso-α scale vortex are conducted as follows.
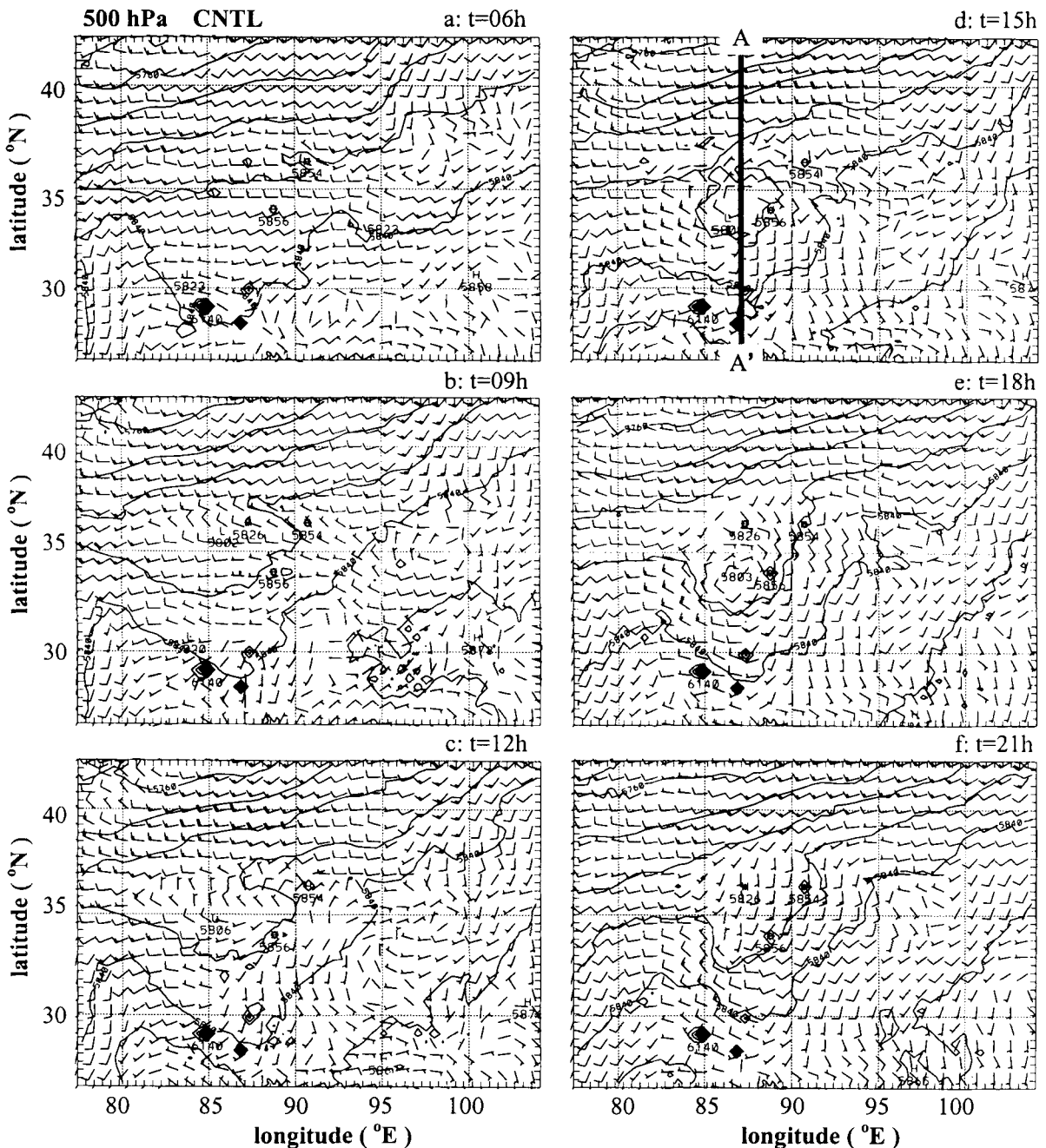
Fig. 5. CNTL-simulated 500 hPa winds (half barb=5 m s^{-1}) and geopotential heights (solid line, 20 gpm intervals) from t=06 h to 21 h every 3 h.

(1) Evolution of the CNTL-simulated meso-α scale vortex

A northwestward little ridge near (36°N, 91°E) showed up in the CNTL-simulated 500 hPa geopotential height field at t=06 h and at this time the model wind field had not yet changed (Fig. 5a). At t=09 h this height ridge became manifest and to its west

along 36°N the wind field changed in wind direction from a westerly to a northwesterly wind (Fig. 5b). At the same time, a visible upstream height trough came out, but the wind field in this height trough remained westerly and had not yet changed at this time. Afterwards, the height trough developed progressively and the wind field in its domain changed greatly to form a

striking east-west shear line of convergence along 35°N and from 85°E to 95°E at $t=12$ h (Fig. 5c); meanwhile, along 86°E and to the south of this wind shear lay another developed wind shear (which was very weak at $t=06$ h). Around the intersection of these two wind shears developed a clear-cut meso-α scale cyclonic vortex with a close contour of 5820 gm at $t=15$ h, which was centered at (34°N, 87.5°E). The vortex was more nearly circular at $t=18$ h, but the close contour vanished and changed into a height trough. And at $t=21$ h, the vortex vanished and became a north-south wind shear.

So this meso-scale cyclonic vortex originated and developed over the plateau. Of striking interest is that the change in geopotential height, which initially occurred near noon, was prior to that in the wind in its whole evolution including the processes of its initial development and its decay. It follows that the vortex

was mainly associated with the thermal effects of the plateau.
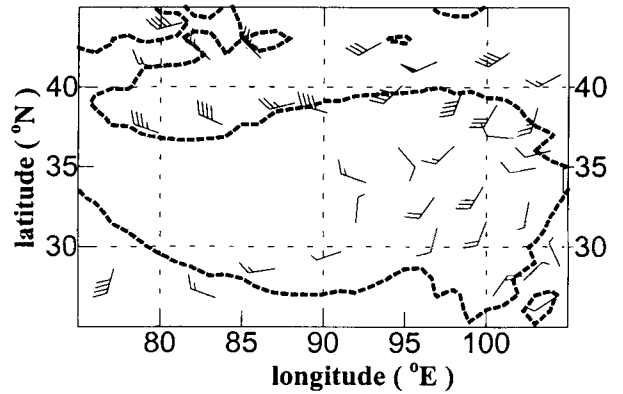
(2) Structure of the CNTL-simulated meso-α scale vortex

Fig. 6. 500 hPa observation winds (half barb=2 m s^{-1}) at 1200 UTC 26 July.
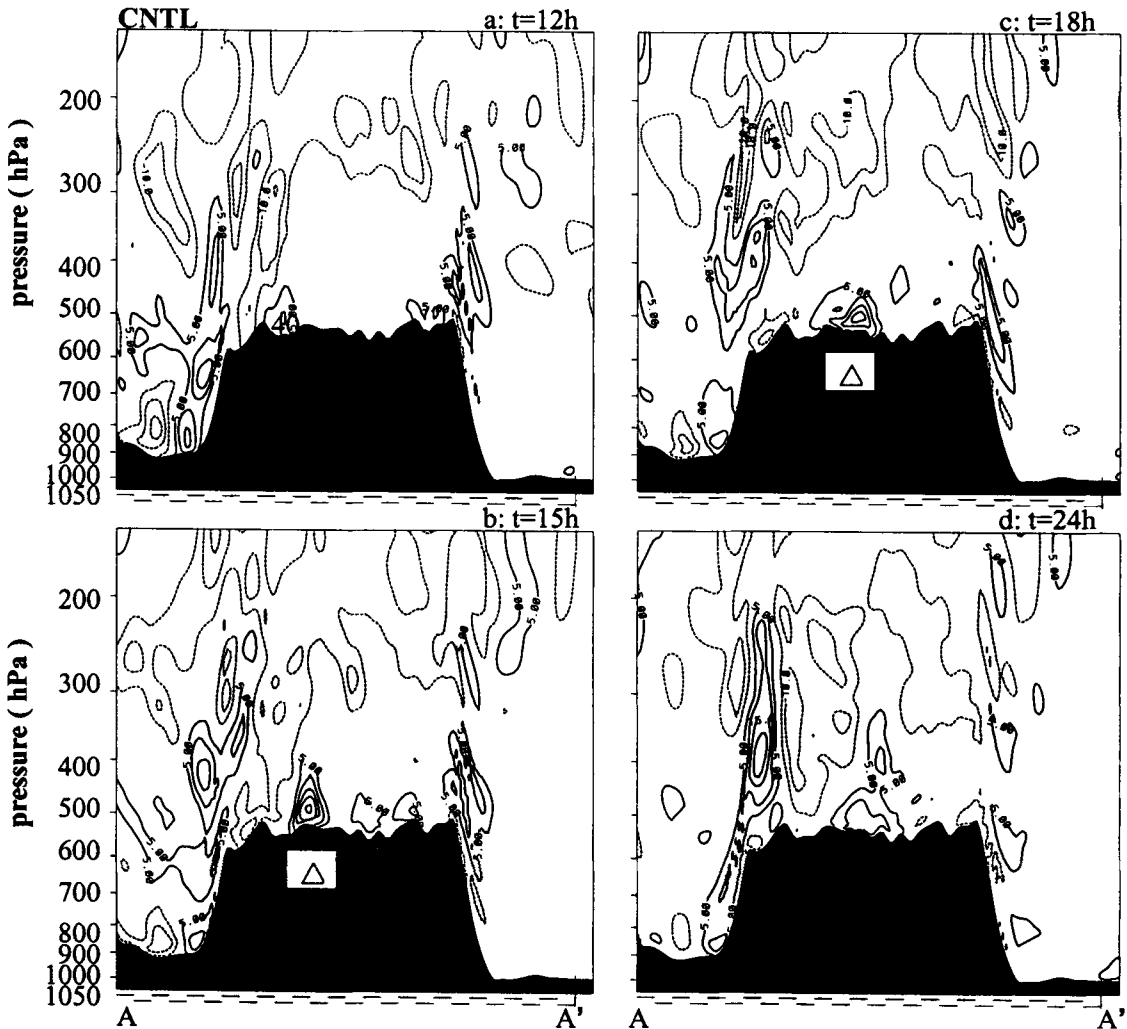
Fig. 7. Vertical cross section of the CNTL-simulated vorticity, taken along line 87°E and through the center of the vortex during $t=12$ h–24 h (5×10^{-5} s^{-1} intervals, negative dashed).

Figures 7 gives the vertical cross sections of the CNTL-simulated vorticity taken along line **AA'** in Fig. 5d, which is through the center of the vortex along 87°E.

It can be seen that the mesoscale cyclonic vortex (in Figs. 7b and c, indicated by △), within an updraft area (figures for vertical cross section of vertical velocity not shown), was confined to the lower troposphere under 450 hPa over the plateau and shrinks its extent with height, with a diameter of 4° longitude at 500 hPa. The plateau was dominated by anticyclonic vorticity above 450 hPa. This mesoscale cyclonic vortex lasted for 3–6 hours and was strong during $t=15$ h–18 h, with a high center of vorticity at 500 hPa and a maximum up to $(25$–$30)\times10^{-5}$ s^{-1}; afterwards it declined (Fig. 7d). And it can be seen that the vortex does not form until the mature stage of the MCS.

In the vertical cross section of vertical velocity (not shown) it can be seen that after $t=09$ h the upward motion became active by solar heating and subsequently became dominant in the troposphere over the plateau; and its range expanded and shifted upward with time. It reached its peak at $t=15$ h and extended above 200

hPa with a maximum of 0.34 m s^{-1} near 400 hPa (below 400 hPa at $t=12$ h). And then the ascending motion over the plateau gradually abated but the area with ascending motion continued to uplift; at $t=21$ h its peak value was reduced to 0.15 m s^{-1}, with its center at 300 hPa; and at this time the downward motion was dominant below 400 hPa over the plateau. It is obvious that the updrafts over the plateau became active at noon, associated with the initial stage of the MCS. The updrafts reached their peak and lasted for several hours after the MCS was mature. The evolution of the updrafts over the plateau reflects that the model displays the features of the MCS associated with the diurnal variation.

4. A series of sensitivity experiments (NRAD, NSEN, FDRY, and NLAT)

The sensitivity experiments include one of the pseudo-adiabatic process (FDRY) and ones regardless of the surface and atmospheric radiations (NRAD), surface sensitive heat (NSEN), and surface latent heat
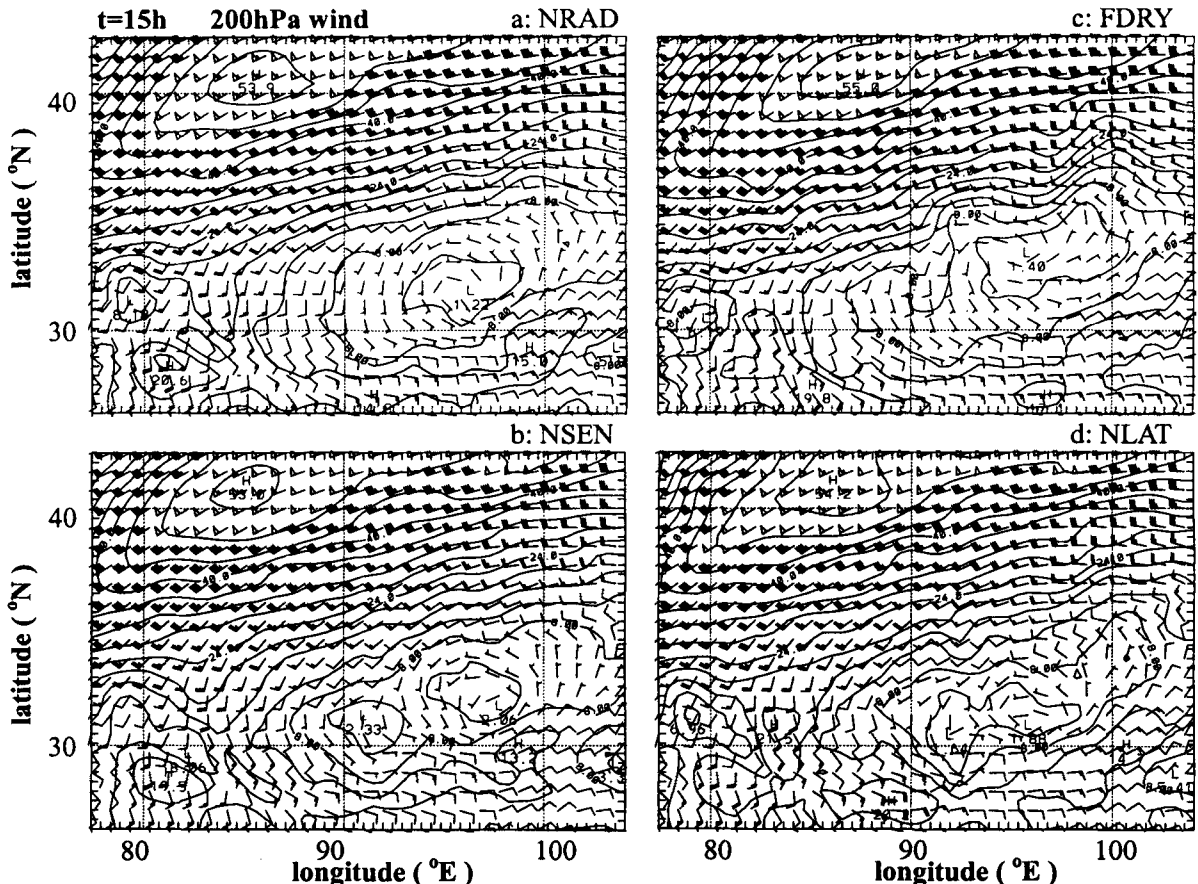

Fig. 8. 200 hPa forecast winds at $t=15$ h simulated by (a) NRAD, (b) NSEN, (c) FDRY and (d) NLAT (thick lines for isotachs, 4 m s^{-1} intervals).

(NLAT), respectively. They are conducted to investigate the impact of various surface thermal forcings and other physical processes on the MCS over the plateau.
(1) Model-simulated 200 hPa wind fields

Because of the lag of 3 hours in the simulation, $t=15$ h from the model integration, although valid for 1500 UTC 26, is virtually denoted 1200 UTC 26 when the MCS involved reached its peak. Figure 8 presents the 200 hPa forecast winds simulated by (a) NRAD, (b) NSEN, (c) FDRY, and (d) NLAT.

The simulated 200 hPa wind fields in Fig. 8 are very similar to those by CNTL in Fig. 2d. That is, the plateau was occupied by a prominent northeast-southwest anticyclone with its center around (32°N, 97°E). Therefore all the sensitivity experiments indicate that the upper-level largescale wind field over the plateau was affected only slightly by the various surface thermal forcings and other physical processes.
(2) Model-simulated 400 hPa rainwater mixing rate

The 400 hPa rainwater mixing rate simulated by NRAD and NLAT reached its peak at $t=15$ h, by NSEN at $t=18$ h, and by FDRY during $t=12$ h–15

h, indicating different temporal lags from these experiments. Figure 9 presents the 400 hPa rainwater mixing rate simulated by the different experiments at their peak.

Among them, the rainwater mixing rate over the plateau was weakest from NRAD (Fig. 9a) just with some scattered small rainwater areas and with untrue locations compared with the T_{bb} map at 1200 UTC (Fig. 4d). Moreover, the rainwater associated with the westerly trough on the northwestern edge of the plateau appeared even at $t=18$ h (figure not shown). It follows that the simulation of the rainwater was affected badly by NRAD.

The simulated rainwater from NSEN was very weak especially over the plateau, for example, having no meso-β scale rainwater belts in Fig. 9b (marked A1, A2, A3, and B2 in Fig. 4b for CNTL), and with a temporal lag longer than CNTL's. However, the simulated westerly rainwater from NSEN was nearly similar to that from CNTL. This experiment suggests that the surface sensitive heat flux is very important to the development of the MCS over the plateau.
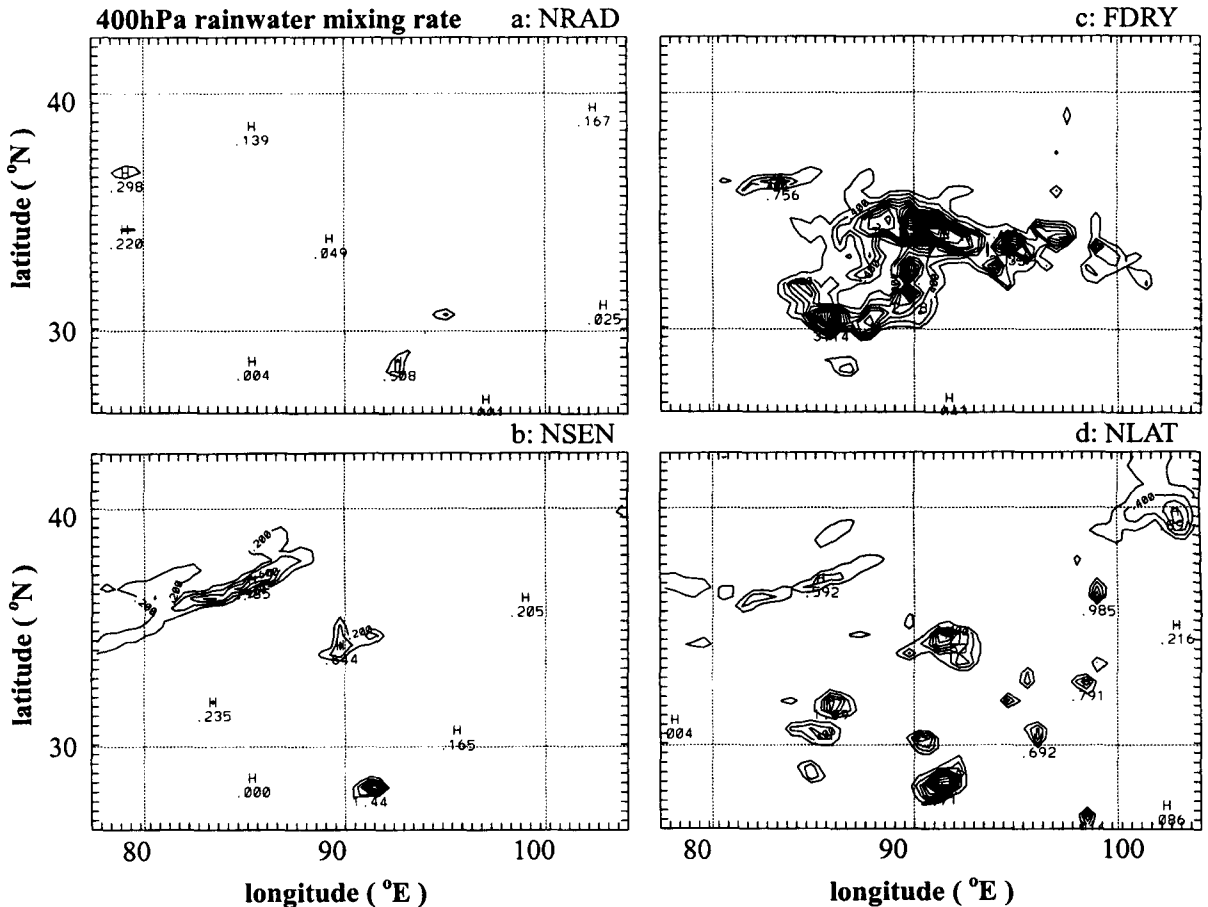

Fig. 9.   400 hPa rainwater mixing rate (0.2 g kg^{-1} intervals) from NRAD, NSEN, FDRY and NLAT at their peak (all at $t=15$ h, except for NSEN, $t=18$ h).
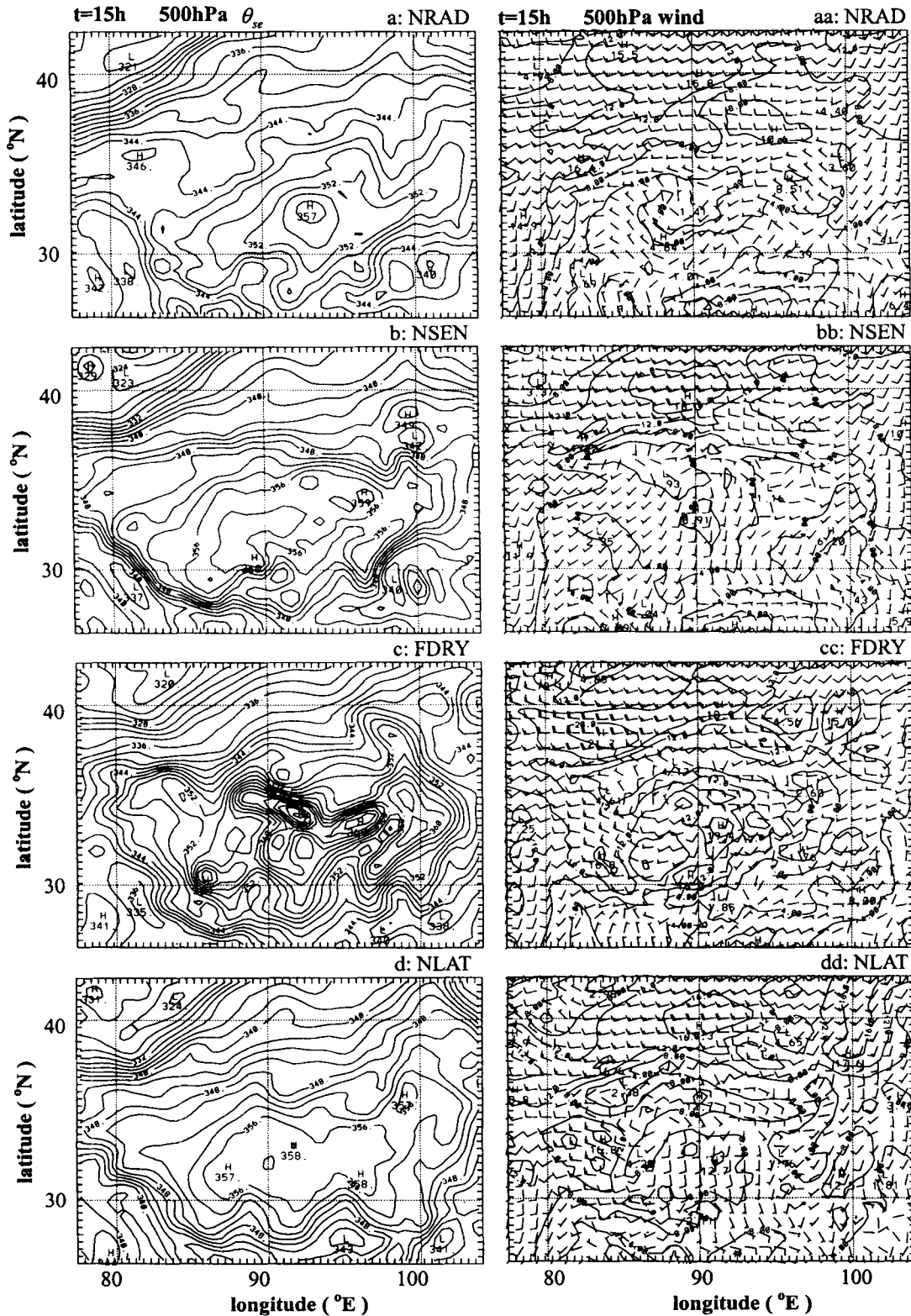
Fig. 10. Simulated 500 hPa winds (thick lines for isotachs, 4 m s^{-1} intervals) and θ_{se} (2 K intervals) by NRAD, NSEN, FDRY and NLAT at t=15 h.

FDRY notably strengthens the simulated rainwater over the plateau, with an expanded rainwater area (Fig. 9c) compared with CNTL (Fig. 4b). Furthermore, the FDRY rainwater area over the plateau was something similar in shape to the MCS in the T_{bb} map (Fig. 4d), although haveing a northwestward deflection in position. So taking the pseudo-adiabatic process (FDRY) into consideration can improve the simulation of the MCS over the plateau in some aspects, which reflects a certain facticity and rationality of the pseudo-adiabatic process in the development of the MCS over the plateau.

The simulated rainwater from NLAT (Fig. 9d) was very similar to that from CNTL (Fig. 4b). This indicates that the surface latent heat flux is of little importance to the development of the MCS over the plateau.

(3) Model-simulated 500 hPa winds and θ_{se}

Because it is known in the above Subsection 1 that the upper-level largescale wind field over the plateau differed slightly in the experiments of NRAD, NSEN, FDRY, and NLAT, causes should be evident in the lower layers which were responsible for the difference among these experiments described in the above subsection 2. Figure 10 shows the simulated 500 hPa winds and θ_{se} at $t=15$ h by NRAD, NSEN, FDRY, and NLAT.

As in the above subsection 2, the NRAD-simulated 500 hPa θ_{se} over the plateau was weakest in Fig. 10a with its range of contours 352 K much less than that of contour 356 K from CNTL (Fig. 4a), and with an eastward deflection in position. In addition, the 500 hPa low θ_{se} area associated with the westerly trough on the northwestern edge of the plateau was less notable and therefore there was a weaker θ_{se} gradient in the northwest of the plateau from NRAD than from CNTL. In the aspect of the 500 hPa wind field, NRAD produced just a northeast-southwest wind shear over the central plateau (Fig. 10aa) located on the northwestern edge of the high θ_{se} center, and not a mesoscale cyclonic vortex previously described in section 3.3. As the case stands, NRAD greatly weakened the 500 hPa winds and θ_{se} compared with CNTL.

Compared with the CNTL-simulated θ_{se} (Fig. 4a), the NSEN-simulated high θ_{se} area over the plateau in Fig. 10b had a visible westward deflection in position with its center located west of 90°E, opposite to the above case of NRAD. NSEN did not produce the meso-scale cyclonic vortex at 500 hPa associated with the MCS. However, different from NRAD, NSEN produced just an east-west wind shear along 35°N and from 87°E to 93°E (Fig. 10bb).

It can be deduced from the comparison of NRAD with NSEN based on CNTL that these two physical processes of the surface and atmospheric radiations

and surface sensitive heat over the plateau had somewhat an opposite but equivalent role in the evolution of the MCS involved.

The FDRY-simulated 500 hPa θ_{se} over the plateau was the strongest among all of the experiments in Fig. 10c, and it was closer to the θ_{se} analysis (Fig. 4c) than CNTL's in magnitude and distribution pattern. In the FDRY-simulated 500 hPa wind field (Fig. 10cc) appeared the meso-scale cyclonic vortex associated with the MCS involved, which was to the east of the CNTL-simulated vortex (Fig. 5d) and so had a smaller position deflection from the wind analysis (Fig. 6) than the CNTL-simulated one.

It is the same case for the NLAT-simulated 400 hPa rainwater mixing rate, described in the above subsection 2, that the NLAT-simulated 500 hPa θ_{se} and winds in Fig. 10d and Fig. 10dd were very similar to those by CNTL (Fig. 4a and Fig. 5d). This reveals that the surface latent heat flux was of little importance to the development of the MCS involved.

5. Summary

It is a challenging attempt to simulate the MCSs over the plateau with a mesoscale numerical model. In this study, the fifth version of the Penn State-NCAR nonhydrostatic mesoscale model (MM5) is employed for a numerical study of a MCS developing over the Qinghai-Xizang plateau on 26 July 1995. The results are inspiring and are summarized below.

(1) The model reproduces the largescale conditions in which the MCS concerned is embedded, which are the well-known anticyclonic Qinghai-Xizang Plateau High in the upper layers and the strong thermal forcing in the lower layers.

The model captures the meso-α scale vortex associated with the MCS, which can be analyzed in the observational 500 hPa winds. And to some degree, the model reproduces even the meso-β scale substructure of the MCS represented in the model rainwater at 400 hPa, which is similar to satellite images.

On the other hand, there are some distinct deficiencies in the model simulation; for example, the simulated MCS occurs with a lag of 3 hours and a westward deviation of 3–5° longitude.

The structure and evolution of the simulated meso-α scale vortex are undescribable for upper-air sounding data. The vortex is confined to the lower troposphere under 450 hPa over the plateau and shrinks its extent with height, with a diameter of 4° longitude at 500 hPa. It is within the updraft area, but with an anticyclone and downdraft in the upper layers over it. The vortex originates over the plateau, and does not

form until the mature stage of the MCS. It lasts for 3–6 hours. In its processes of both formation and decay, the change in geopotential height field is prior to that in wind field. It follows that the vortex is closely associated with the thermal effects over the plateau.

(2) Then a series of sensitivity experiments are conducted, including NRAD (without surface and atmospheric radiations), NSEN (without surface sensitive heat), FDRY (with pseudo-adiabatic process), and NLAT (without surface latent heat).

The simulated upper-level large-scale wind fields over the plateau differ little from each other for all of these experiments. This indicates that the upper-level large-scale wind field was affected slightly by the various surface thermal forcings and other physical processes.

It is clearly documented that there is close relation between the 400 hPa rainwater and the 500 hPa θ_{se}.

Among all these experiments, NRAD has the worst impact on the MCS over the plateau; NSEN is next to NRAD. In both of these simulations, the θ_{se} is weak in the lower layers over the plateau and the meso-α scale vortex associated with the MCS cannot come out over the plateau. Of meaningful interest is that NRAD and NSEN have somewhat an opposite but equivalent effect, with a 500 hPa high θ_{se} center east of 90°E for NRAD but west of 90°E for NSEN and just a northeast-southwest wind shear over the central plateau for NRAD but an east-west wind shear over the northern plateau for NSEN in the 500 hPa wind field.

FDRY can improve the simulation of the MCS over the plateau in some aspects, and so taking the pseudo-adiabatic process into consideration may reflect a certain facticity and rationality in the development of the MCS over the plateau.

The simulation of NLAT is very similar to that of CNTL. Therefore the surface latent heat flux is of little importance to the development of the MCS over the plateau.

It can be concluded that under the background conditions of the upper-level anticyclonic Qinghai-Xizang Plateau High, the MCS involved is mainly dominated by the low-level thermal effects over the plateau including surface and atmospheric radiations, surface sensitive heat, and the pseudo-adiabatic process. The simulation described here is a good indication that it may be possible to reproduce the MCS over the plateau under certain large-scale conditions and with the incorporation of proper low-level ther-

mal physics.

6. Discussion

The analysis in Zhu and Chen (1999) shows the fact of the great upper-level Qinghai-Xizang anticyclonic high and the strong low-level thermal forcing where the MCS over the plateau on 26 July developed. These facts are so outstanding that we come to suggest that they are the possible and potential reason for the current attempt to simulate the MCS rather successfully. It also shows that the great Qinghai-Xizang Plateau anticyclonic high had the MCS in the current case affected little by the westerlies and the MCS developed in the central section within the warm and moist area in the low layers (refer to Fig. 5 in Zhu and Chen, 1999); and therefore there was a weak link to the physical processes of baroclinicity and temperature advection in its development. Furthermore, as we have seen, the great Qinghai-Xizang Plateau anticyclonic high in the upper layers and the strong thermal forcing in the lower layers are intimately linked with the thermal effects of the plateau. So the development of this MCS may be mainly associated with the relatively pure thermal effects peculiar to the Qinghai-Xizang Plateau. This implies that the Qinghai-Xizang Plateau may be a special and meaningful platform for research on large MCSs.

The current case study also supports a common conclusion of Madox (1983), Velasco and Fritsch (1987), Cotton et al. (1989), and Augustine and Howard (1991) that MCCs (circular and large MCSs) are primarily driven by low-level thermal forcing and conditional instability. Obviously, this common conclusion aims at the low-level meteorological conditions associated with MCCs. On the other hand, there have been different findings with regard to midlevel to upper meteorological conditions associated with MCCs. The 10-case storm-relative composite of Madox (1983) resolved a weak, midlevel short-wave trough upstream of the MCC development area, but the larger-sample composite of Cotton et al. (1989) did not show this. The census of Velasco and Fritsch (1987) and Augustine and Howard (1991) found that MCCs tend to congregate on the periphery of a largescale midlevel anticyclone. In the present study, the great anticyclonic Qinghai-Xizang Plateau high in the upper layers was the background condition of the large MCS. Based on Blanchard et al.'s work (1998) on mesoscale circulation growth under conditions of weak inertial instability, we may come to another common conclusion that circular and large MCSs are generally developed under the background condition of weak inertial instability

in the midlevel to upper layers, although with various patterns.

REFERENCES

Anthes, R. A., Y. -H. Kuo, S. G. Benjamin, and Y. -F. Li, 1982: The evolution of the mesoscale environment of severe local storms: Preliminary modeling results. *Mon. Wea. Rev.*, **110**, 1187–1213.

Augustine, J. A., and K. W. Howard, 1991: Meso-scale convective complexes over the United States during 1986 and 1987. *Mon. Wea. Rev.*, **119**, 1575–1589.

Blanchard, R. O., W. R. Cotton, and J. M. Brown, 1998: Mesoscale circulation growth under conditions of weak inertial instability. *Mon. Wea. Rev.*, **126**, 118–140.

Cotton, W. R., M. -S. Lin, R. L. McAnelly, and C. J. Tremback, 1989: A composite model of meso-scale convective complexes. *Mon. Wea. Rev.*, **117**, 765–783.

Grell, G. A., J. Dudhia, and D. R. Stauffer, 1994: A description of the fifth generation Penn State/NCAR mesoscale model (MM5). NCAR Tech. Note, NCAR/TN-398+STR, 138pp.

Kain, J. S., and J. M. Fritsch, 1993: Convective parameterization for mesoscale model: The Kain-Fritsch scheme. The Representation of Cumulus Convection in Numerical Models. *Meteor. Monogr.*, No 46, Amer. Meteor. Soc., 165–170.

Maddox, R. A., 1980: Meso-scale convective complex. *Bull. Amer. Meteor. Soc.*, **61**, 1374–1387.

Maddox, R. A., 1983: Large-scale meteorological conditions associated with midlatitude, meso-scale convective complexes. *Mon. Wea. Rev.*, **111**, 1475–1493.

Velasco, I., and J. M. Fritsch, 1987: Mesoscale convective complexes in the Americas. *J. Geophys. Res.*, **92**, 9591–9613.

Zhang, D.-L., and R. A. Anthes, 1982: A high-resolution model of the planetary boundary layer-sensitivity tests and comparisons with SESAME-79 data. *J. Appl. Meteor.*, **21**, 1594–1609.

Zhang, D. -L., K. Gao, and D. B. Parsons, 1989: Numerical simulation of an intense squall line during 10-11 June 1985 PRE-STORM. Part 1: Model verification. *Mon. Wea. Rev.*, **117**, 960–994.

Zhu G. F., and Chen S. J., 2003: Analysis and comparison of mesoscale convective systems over the Qinghai-Xizang (Tibetan) Plateau. *Advances in Atmospheric Sciences*, **20**, 311–322.

青藏高原上中尺度对流系统(MCS)的数值模拟

朱国富　　陈受钧

摘　要

采用MM5非静力原始方程中尺度模式模拟了1995年7月26日发生在高原上的中尺度对流系统(MCS)。(1)模式基本上模拟出26日高原上MCS发生发展的大尺度背景场，它们是强大的对流层高层青藏高原反气旋高压和强的低层热力强迫。模式还得到了与MCS相联的α中尺度涡旋，它能在500 hPa实测风场中得到反映，而且，模式模拟的400 hPa雨水混合比场在一定程度上模拟了MCS在T_{bb}图上反映的β中尺度次级结构特征。另一方面，模拟存在的差异也是明显的，例如：时间上有3小时滞后；模拟的MCS α中尺度涡旋位置偏西3-5个经度。(2)模拟的α中尺度气旋性涡旋的结构和演变是高原上探空资料难于描述的。模拟的结果表明，它只限于高原上在450 hPa以下的对流层中低层，范围向上减小，在500 hPa直径约4个经纬度。这个中低层涡旋对应上升运动区，但它的上方是反气旋涡度，对应下沉运动。该涡旋是在高原上从无到有发展出来的，出现在MCS成熟阶段和之后，持续3-6个小时。在它的形成和消亡时都是位势高度场的变化先于风场的变化，这表明该涡旋与高原上的热力作用密切相联。(3)一系列模式敏感性试验考察了不同的物理过程和高原地表热力强迫对高原上MCS的影响。结果表明，文中的高原上MCS在高层青藏高原反气旋高压的大尺度背景下主要受中低层热力强迫的支配。这些模拟结果暗示出一定的高层大尺度背景下适当的低层热力效应就有可能在高原上形成MCS的可能性。

关键词：青藏高原, 中尺度对流系统(MCS), 数值模拟